From an ellipsoid-based to an anthropomorphic articulated total body model for multibody applications

Pascoletti, G.; Huysmans, T.; Molenbroek, J.F.M.; Zanetti, E.M.

DOI
10.1007/s12008-023-01427-0

Publication date
2023

Document Version
Final published version

Published in
International Journal on Interactive Design and Manufacturing

International Journal on Interactive Design and Manufacturing (IJIDeM) (2024) 18:5991–6011
https://doi.org/10.1007/s12008-023-01427-0

ORIGINAL PAPER

From an ellipsoid-based to an anthropomorphic articulated total body model for multibody applications

G. Pascoletti[1] · T. Huysmans[2,3] · J. F. M. Molenbroek[2] · E. M. Zanetti[1]

Received: 29 July 2022 / Accepted: 26 June 2023 / Published online: 25 July 2023

Abstract
Human computer models represent a useful tool for investigating the human body response to external static/dynamic loads or for human-centred design. Articulated Total Body (ATB) models are the simplest human multibody models, where body segments are represented by ellipsoids joined at skeletal articulations. Over the years, regression models on both living subjects' and cadavers' data have been developed to predict body segments properties. These models are affected by two main limitations: the only inputs are the subject's weight and height, not considering that for the same combination different morphologies can exist; secondly, regression analyses were performed over a specific population not including peculiar morphologies (under-weight or obese). A novel methodology for developing anthropomorphic ATB models is here presented: a statistical shape model able to predict the external geometry of the human body from a limited set of anthropometric measurements was implemented and body segments were obtained by segmentation; the respective inertial properties were computed from volumes, assuming a constant density value. The properties of this new anthropomorphic ATB model were compared to those calculated by GEBOD (Generator of Body Data), a well-known programme for ATB data calculation. A virtual population of twenty subjects was analysed: with reference to the inertial properties the most relevant differences occurred at the abdomen and the thighs segments (60% relative error), while the trunk, the shoulder and the calves represent the most critical areas for the geometry reconstruction (50 mm average error). The significance of these outcomes was investigated performing multibody simulations with various scenarios.

Keywords Multibody modelling · Articulated total body model · Principal component analysis · Accident · Forensic biomechanics · CAESAR database

1 Introduction

Numerical human body models have the main aim of replicating the actual mechanical behaviour of the human body as accurately as possible. They can be used to investigate various biomechanical aspects, such as joint and muscle forces, risks of musculoskeletal injuries, kinetic motion analyses, impact dynamics, and to be a valid support for human-centred design or injury reconstruction analyses [1–3]. Articulated Total Body (ATB) models are numerical models composed by rigid bodies (typically ellipsoids) joined at skeletal articulations; they represent a useful tool for biomechanical numerical analyses, thanks to the low computational effort required and the ability of providing human body kinematic response to static and dynamic load scenarios [4].

To make this possible, an accurate estimate of human body segments parameters is required: mass, principal moments of inertia, centre of mass location and external geometry are the fundamental inputs for the human body model creation.

Historically, many different techniques have been investigated to obtain body segments parameters, including analyses on both living subjects and cadavers [5]. For instance, widely used procedures were the immersion method [6] or photogrammetry [7] for segments' volume definition, as well as the quick release [8] or the compound pendulum [9] methods for moments of inertia and centres of mass assessment.

✉ G. Pascoletti
giulia.pascoletti@unipg.it

1 Department of Engineering, University of Perugia, 06125 Perugia, Italy

2 Section of Applied Ergonomics and Design, Department of Human Centered Design, Faculty of Industrial Design Engineering, Delft University of Technology, Delft, The Netherlands

3 imec-Vision Lab, Department of Physics, University of Antwerp, Antwerp, Belgium

Other authors have carried out extensive experimental activities, based on cadaver [6, 10–13] or imaging data [14–17], whose output was the definition of regression models able to predict body segments' parameters, having the height and the mass of the subject as inputs. The main issue related to these models is that the specific population over which the regression was performed must be representative of the whole population; this could represent a limitation when peculiar morphologies are being inquired, such as overweight, obese, or under-weight subjects [18, 19]. Moreover, cadaver studies are often carried out on a limited number of elder subjects, therefore it is not possible to consider changes of parameters versus age. As general rule, the application of these regression coefficients outside the population over which they have been obtained must be done cautiously, as it could lead to errors. In addition, regression models are usually based on a very limited number of input variables (for example the only weight and height), therefore, they do not take into account that, given the same combination of input parameters, different morphologies can exist, leading to an approximate representation of morphology and mass/inertias distribution. This aspect can represent a critical issue when the numerical human model is intended for being part of an interactive design environment for human-centred analyses [20–23]. Indeed, the interactive approach is based on the definition of a numerical model able to represent the actual features of the subject under consideration, in order to perform subject-specific kinematic or dynamic analyses, or customised device design and assessment.

One of the most used program for ATB properties generation is the so called "Generator of Body Data" (GEBOD) [24–26], which determines dimensions and inertial parameters of ellipsoids, corresponding to a specific subject, through regression laws having gender, age, weight and/or height data as independent variables; these regression equations were derived from human stereophotogrammetric data collected by McConville et al. [17] and Young et al. [27].

In the last few years, there was a growing interest toward the application of new and advanced technologies to measure body segments properties and provide more accurate surface and inertial data [2, 28, 29], in order to overcome the above outlined limitations. Actually, many different works report the relevance of the application of 3D laser scanning [29, 30], X-ray [28], dual energy X-ray absorptiometry (DEXA) [1, 2], CT scan [31], 3D photogrammetry [32] techniques as reliable methods to improve human body geometry reconstruction and evaluate, directly or indirectly, body segments parameters for individualized biomechanical models.

In this work, a different approach was followed, leading to build a multibody (MB) ATB model with an anthropomorphic geometry. The novelty of the methodology here proposed is the use of a Statistical Shape Model (SSM) able to generate the 3D external geometry of the human subject knowing few anthropometric measurements and with a very limited deviation from the actual human shape (9.24 $\pm$ 2.25 mm [33]). The ATB multibody model was generated from this 3D shape, using anatomical planes for segmenting the whole-body geometry into body segments. These geometries could be directly imported into the multibody code (MSC Adams, MSC Software Corporation rel. 17) and the respective mass, principal moments of inertia and centre of mass location were obtained under the assumption of a uniform density [34]. Lastly, the segments were articulated to one another by means of mechanical joints (revolute or spherical), and passive resistive properties were defined to prevent non-physiological motions [35, 36]. The anthropomorphic inertial and geometrical properties are reasonably expected to be less affected by limitations typical of the regression-based models, given the high accuracy of the SSM in replicating the actual human shape [37].

The evaluation of anthropomorphic ATB model was conducted by comparing its outputs to GEBOD datasets, as the last ones are still being widely used in the common practice, thanks to the wide diffusion of the respective regression equations in literature [24–26] and in many software. ATB models have been compared in terms of inertial properties, outer 3D external geometry of body segments and anatomical joint locations. On completion of this work, the significance of these findings has undergone further investigation through the use of multibody simulations, where a subject with a less common external geometry (obese subject) was investigated. This multibody analysis was aimed to assess the relevance of inertial and geometrical differences found from the previous analyses within output results of dynamic models.

2 Materials and Methods

A comprehensive overview of the classical ATB ellipsoids-based model is provided in Sect. 2.1 and a detailed description of the proposed innovative anthropomorphic human modelling approach is reported in Sect. 2.2. A sample set of 20 adult males was selected and both anthropomorphic and multi-ellipsoid models were generated for each individual (Sect. 2.3).

Each ATB model was made of fifteen segments: according to the most common configuration in literature, the hands and forearms were joined together in one single segment (Sect. 2.1). The list of these segments and the respective representation is shown in Fig. 1.

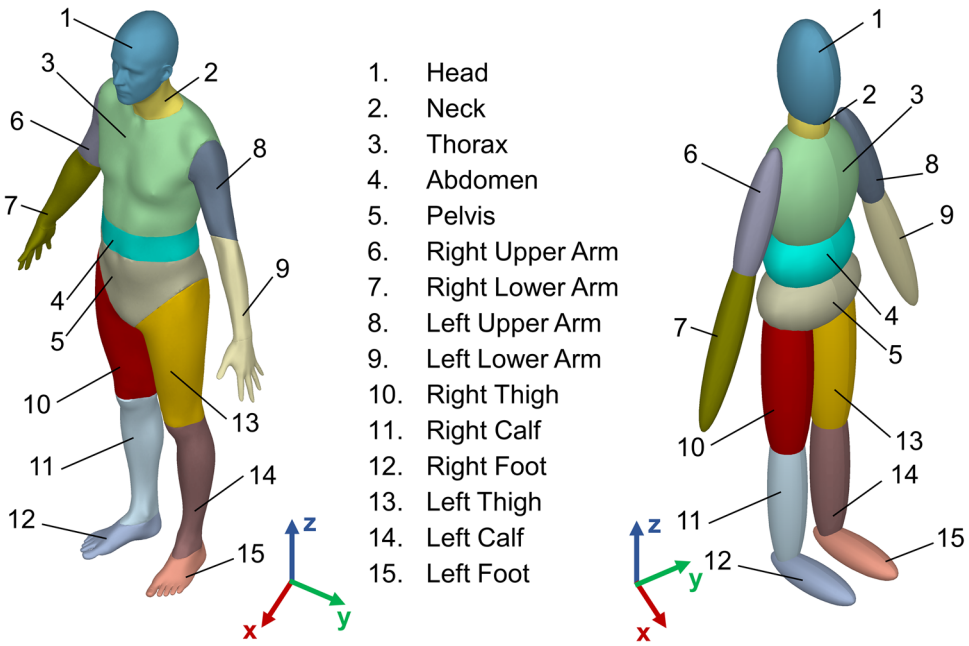

Fig. 1 Body segments for the anthropomorphic and the multi-ellipsoids ATB models

2.1 Multi-ellipsoids Model

The Generator of Body Data (GEBOD) software is considered a gold-standard tool for generating human datasets for multibody analyses; it was developed by the United States Air Force Research Laboratory for the creation of human and dummy body dimensional (external geometry) and inertial properties datasets [24, 25]. This program was born in the 80–90s and thereafter it was a reference for geometrical and inertial data of human subjects to be implemented in multibody analyses [38, 39].

In this software, body segments were modelled as rigid bodies represented by ellipsoids that were joined to one another at locations corresponding to human body's articulations. The ATB model could be made of fifteen to seventeen ellipsoids, depending on whether the lower arm and the hand segments were joined or not. The configuration consisting of fifteen segments (Fig. 1) was selected for the following comparison analyses, due to its widespread use in the field.

Each segment was assigned a given geometry (semiaxes of ellipsoids) and inertial properties, which were computed from GEBOD regression equations. It should be here stressed that these equations actually come from anthropometric surveys [40–42] and stereophotogrammetric data [17, 27] performed over a limited population, both in terms of number of subjects (46 females and 31 males) and variety of morphologies (United States Air Force flying population). Regression equations follow a general form as stated in Eq. 1. The predicted variable can either be a geometrical or inertial property, while the model inputs are the weight and height of the human subject. Depending on the gender (male or female) and age (adult or child), various sets of equations are available. In Eq. 1, the regression coefficients are represented by e, f, and g:

$$\text{Predicted Variable} = (\text{e} * \text{Weight}) + (\text{f} * \text{Height}) + \text{g} \quad (1)$$

Specifically, the following variables could be predicted:

- Segment size:
  - Semiaxes of ellipsoids approximating the segment geometry.
- Segment inertial properties:
  - Volumes.
  - Centre of mass location.
  - Principal moments of inertia.
- Joint centre location.

These regression equations are thoroughly documented in the GEBOD manuals [24–27]. The code required to generate the ellipsoids model was implemented into MATLAB (v. 17, The MathWorks, Inc., Natick, MA, USA); finally, the predicted geometrical and inertial data were imported into the multibody code.

For what concerns the mass distribution within the body, the GEBOD program assumed that the human body was homogeneous; each body segment was therefore assigned the same constant density value (1000 kg/m^3 [24]). The estimated volumes, obtained from regression equations, allow

computing each segments' mass as:

$$m_i = v_i \cdot \rho \tag{2}$$

where m_i and v_i are the mass (kg) and the volume (m^3) of the i-th segment and ρ (kg/m^3) is the total body density.

2.2 Anthropomorphic model

The anthropomorphic ATB model here proposed was an articulated total body model made of fifteen segments, whose external geometry had an anthropomorphic shape able to accurately replicate the actual body shape (Fig. 1). The whole-body 3D geometry was generated through the implementation of a Statistical Shape Model (SSM), that is a statistical model capable of predicting a new shape through the application of a variability model on an average shape. The code for the implementation of this SSM was created at the Delft University of Technology [43] based on a training set of over 1140 3D human scan data (622 females and 518 males) belonging to the CAESAR (Civilian American And European Surface Anthropometry Resource) database [44]; demographics about this dataset were reported in the Online Resource 1. Here only the main steps of the procedure are presented and a more comprehensive description can be found in [33, 37, 43, 45].

The SSM was defined as follows:

$$\boldsymbol{X}_p = \bar{\boldsymbol{X}} + \boldsymbol{P}\boldsymbol{b} \tag{3}$$

where $\boldsymbol{X}_p$: is the new predicted shape (the human body geometry in this case), $\bar{\boldsymbol{X}}$: is the average shape of the 3D training set (human shapes dataset), $\boldsymbol{P}\boldsymbol{b}$: is the variability model.

The average shape $\bar{\boldsymbol{X}}$ (Eq. 4) was computed by the Generalised Procrustes Analysis (GPA) [46], applied iteratively on the training set composed by N 3D human shapes $\boldsymbol{X}_t$ (point clouds from laser scans):

$$\bar{\boldsymbol{X}} = \frac{1}{N}\sum_{t=1}^{N} \boldsymbol{X}_t \tag{4}$$

The variability model was based on the Principal Component Analysis (PCA): PCA computes the so-called Principal Components (PCs) as the eigenvectors of the covariance matrix of the deviation from the average shape of all shapes belonging to the training set. These eigenvectors are column vectors of matrix $\boldsymbol{P}$ and represent the modes of deformation that the human shape can undergo; the first 40 principal components were retained, which accounts for the 98% of the total variance. As shown in Eq. 3, the PCs were linearly combined through a set of coefficients $\boldsymbol{b}$ (weights), modulating the deformations to be applied to the average shape according to the following relation:

$$\boldsymbol{b} = \boldsymbol{M}\boldsymbol{f} \tag{5}$$

Vector $\boldsymbol{f}$ is the so-called feature vector ($\boldsymbol{f} = [f_1, f_2, \ldots, f_F, 1]^T$) whose elements f_i are the F anthropometric measures selected to deform the average shape; vector f was related to the vector $\boldsymbol{b}$ through a mapping matrix $\boldsymbol{M}$ which was built from the principal components weights matrix ($\boldsymbol{B} = [\boldsymbol{b}_1, \boldsymbol{b}_2, \ldots, \boldsymbol{b}_n]$) and the feature matrix ($\boldsymbol{F} = [\boldsymbol{f}_1, \boldsymbol{f}_2, \ldots, \boldsymbol{f}_n]$) through least squares linear regression, being n the number of principal components (for more details please refer to [33, 47]).

The SSM shape model allows obtaining the anthropomorphic external geometry of the subject being modelled, but further steps are required to obtain an ATB model. Firstly, the 3D geometry must be segmented into 15 closed volumes, each corresponding to a distinct body segment. Next, connectivity matrices must be created and inertial properties assigned to each segment. Finally, the position and properties of joints between segments corresponding to articulations must be established (14 joints for a total of 26 degrees of freedom). The segmentation process was carried out using scripts implemented by the authors in MATLAB, setting up an automatic procedure which had as input the entire external body geometry and provided as output the anthropomorphic geometries of each segment. The main phases of the procedure are outlined in Fig. 2: the first step consists in partitioning the segments' nodes over the average shape, next the nodes over the predicted shape are partitioned; finally, connection matrices are defined for each segment's geometry. The scripts require the external geometries of both the average body shape and the predicted shape to carry out this process, along with identification numbers (IDs) of nodes corresponding to anatomical landmarks. The partition of nodes among body segments was carried out once on the average shape geometry, while the connection matrices of the nodes were computed for each segment on the specific predicted shape. This approach prevented difficulties in the automatic partition of segments for geometries reproducing over-weight subjects, where some flesh margins of the upper arms and the thighs could overlap. Body segments were defined in the same way as those implemented in stereophotometric data in the GEBOD program [17, 27], defining a total of 14 segmenting planes based on anatomical landmarks position (Fig. 2a). These same landmarks are included in the CAESAR documentation [44] and corresponding nodes' IDs were retrieved for the average shape. Segments were defined as the set of nodes lying between two or more of these planes: each point cloud was identified through the dot product between the segmenting plane normal vector and vectors connecting average shape nodes to a point lying on the plane. The average shape and the predicted shape were characterised by iso-topological meshes

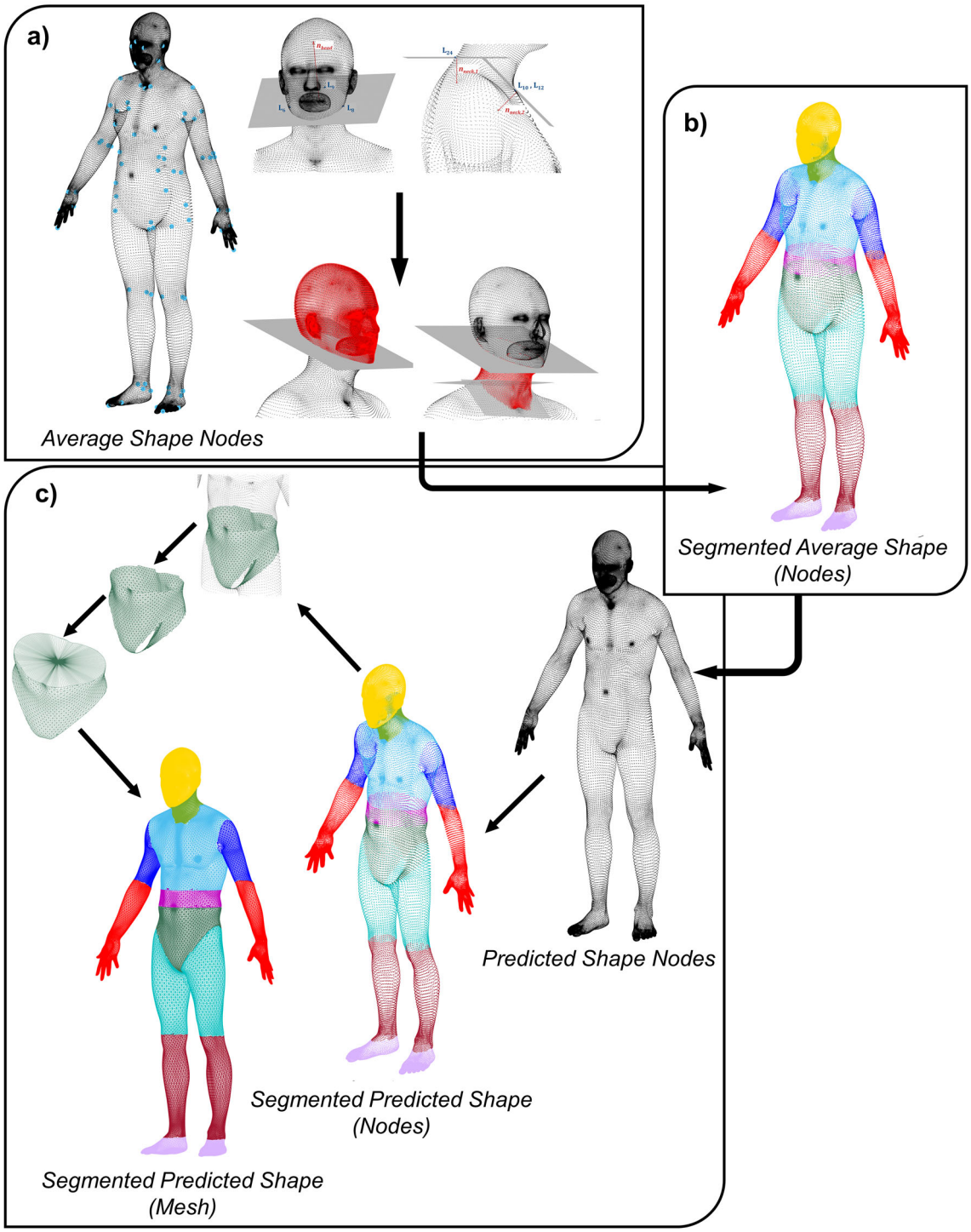

Fig. 2 Segmentation process of the predicted anthropomorphic geometry

(also referred to as homological meshes), that are meshes with the same number of nodes and with nodes representing the same geometrical point; therefore, once segments' point clouds had been identified on the average shape (Fig. 2b), also the nodes identification number was known and the segmentation could be extended straightforwardly to every predicted shape (Fig. 2c).

Finally, the connectivity matrix of each segment was obtained from the full connectivity matrix of the average surface, searching for the same node identifier as in the segment set and retrieving the respective connections. In this way, the mesh representing the lateral surface of each segment was obtained. However, end surfaces needed to be added, in order to achieve a manifold solid geometry. To accomplish this, new mesh triangles were created by linking boundary nodes (nodes located on the mesh boundary) to intermediate nodes (new nodes defined as the geometrical centre of the mesh boundary profile). At the end of this process, every segment geometry was fully defined by a set of nodes and the respective connection matrix, that were exported in CAD format (obj) and directly imported into the multibody code (MSC Adams).

A constant density value assumption was made, following a common practice in body segments parameters studies, due to limited density differences between body segments [48–50]. Respective density values were computed for each subject, from the knowledge of the body mass and the total volume of the external geometry. Each segment was assigned this density value, and the corresponding inertial properties were calculated using the multibody software.

The multibody (MB) model was completed by defining the location of the articular joints' using formulations based on anatomical skin landmarks, retrieved from literature [14, 51, 52]. These anatomical points, once identified on the average shape, could be easily transferred to all the predicted shapes, thanks to the one-to-one correspondence between nodes (isotopological meshes).

The accuracy of anthropomorphic external geometries generated by the SSM was assessed and the deviation of the predicted geometry from the actual body scan was very small, being, on average, equal to 9.24 ± 2.25 mm [33]. In light of this, anthropomorphic computed properties (anthropomorphic model properties) were considered as a reference when evaluating the respective deviation from regression-based properties (multi-ellipsoids model properties).

2.3 Sample Subjects

The analysed sample set was composed of 20 male adult subjects, representing a subset of CAESAR database, able to represent a mixed male population with normal-weight, under-weight, over-weight and obese classes. Weights (W) and heights (H) of every subject are reported in Table 1 along with the respective body mass indices BMI and classification:

$$BMI = \frac{W}{H^2} \tag{6}$$

Weight and height data were used as an input to regression equations in multi-ellipsoids models. For what concerns the anthropometric model, the SSM could accept up to 24 measurements as an input; among these, nine measures were selected and used for the external geometry creation, according to findings reported in [33, 37, 45]; they are listed in Table 2.

Examples of the anthropomorphic and ellipsoids geometries for an under-weight, a normal-weight and an over-weight subject are shown in Fig. 3.

Table 1 Sample subjects set: weight, height, BMI and classification

Subject	Weight [kg]	Height [m]	BMI [kg/m^2]	Classification
1	95.0	1.635	35.5	Ob II[d]
2	64.4	1.884	18.1	U[b]
3	108.9	1.812	33.2	Ob I[d]
4	90.0	1.747	29.5	O[c]
5	75.9	1.820	22.9	N[a]
6	103.2	2.017	25.4	N[a]
7	150.0	1.933	40.2	Ob III[d]
8	74.4	1.717	25.2	N[a]
9	75.8	1.860	21.9	N[a]
10	132.0	2.019	32.4	Ob I[d]
11	68.8	1.833	20.5	N[a]
12	86.0	1.896	23.9	N[a]
13	53.6	1.684	18.9	U[b]
14	62.5	1.617	23.9	N[a]
15	122.1	1.874	34.8	Ob I[d]
16	127.5	2.054	30.2	O[c]
17	79.1	1.862	22.8	N[a]
18	85.2	1.849	24.9	N[a]
19	120.0	1.745	39.4	Ob II[d]
20	57.0	1.777	18.1	U[b]

[a]Normal-weight
[b]Under-weight
[c]Over-weight
[d]Obese (with distinction between I class, II class and III class obesity)

Table 2 Anthropometric measures for the SSM

Weight
Stature
Shoulder Breadth
Chest Circumference at Scye
Waist Circumference Preferred
Hip Circumference Maximum
Thigh Circumference
Arm Length
Waist Front Length

2.4 Comparison Analysis

As a first step, the geometry of the ellipsoids-based model was checked against the anthropomorphic model whose accuracy was known from a previous work by some of the authors [33]. The hypothesis was that if the difference between the ellipsoids-based model and the anthropomorphic one was far above this accuracy, assuming the anthropomorphic model and the derived properties as a reference was a reasonable option, as detailed in Sect. 2.4.2.

The following analyses involve a comparison of geometries and inertial properties between the anthropomorphic and multi-ellipsoids ATB models, segment by segment. Additionally, anatomical joint locations were compared for each of the 14 joints. More in detail, investigated parameters for the anthropomorphic or ellipsoids model ($m = A$ or $m = E$ respectively), for every sample subject (s = 1:20), for each specific body segment (b = 1:15) or anatomical joint (j = 1:14) will be reported as:

- $I_{xx,m,s,b}$, $I_{yy,m,s,b}$, $I_{zz,m,s,b}$: principal moments of inertial about x, y and z axis respectively (Fig. 1).
- $M_{m,s,b}$: masses.
- $G_{x,m,s,b}$, $G_{y,m,s,b}$, $G_{z,m,s,b}$: x, y and z (Fig. 1) centres of mass coordinates.
- $J_{x,m,s,j}$, $J_{y,m,s,j}$, $J_{z,m,s,j}$: x, y and z (Fig. 1) articular joints' centre coordinates.

2.4.1 3D external geometry analysis

The ellipsoidal geometry of the entire body was compared to the anthropomorphic 3D shape to assess and quantify the approximation made by former one. The geometrical analysis was performed with 3-Matic software (Materialise, v. 12) through the 'part comparison' analysis tool. The Euclidean nearest neighbour distance approach was used and the distance, in millimetres, between each triangular node of the target shape (anthropomorphic geometry) and the closest triangular node on the surface of the part to be analysed (ellipsoidal geometry) was measured [53]. The analysis has taken into account the maximum, minimum, and mean values, as well as the 10-th and 90-th percentile values.

2.4.2 Statistical analysis of data

Distributions of geometrical errors between models ('*E*' or '*A*') and the 'Actual' geometry, and inertial properties were assumed to follow a normal distribution since they were based on very wide samples (20 subjects multiplied by 79,000 and 35,000 nodes for the anthropomorphic and the multi-ellipsoids models respectively); consequently, with reference to the sum of variances (SS), the following equation holds:

$$SS_{E-Actual} = SS_{E-A} + SS_{A-Actual} \tag{7}$$

when SS_{E-A} is compared to $SS_{A-Actual}$ and the first one is significantly higher (F-test), $SS_{A-Actual}$ is negligible; in this case, the anthropomorphic model can be used as a reference to measure ellipsoids model errors on inertial estimation and joint position estimation.

An F-test was so performed to compare the variance of geometric errors between the ellipsoids model and the anthropomorphic one (σ^2_{E-A}) to the variance of errors between the anthropomorphic model and the actual subject geometry

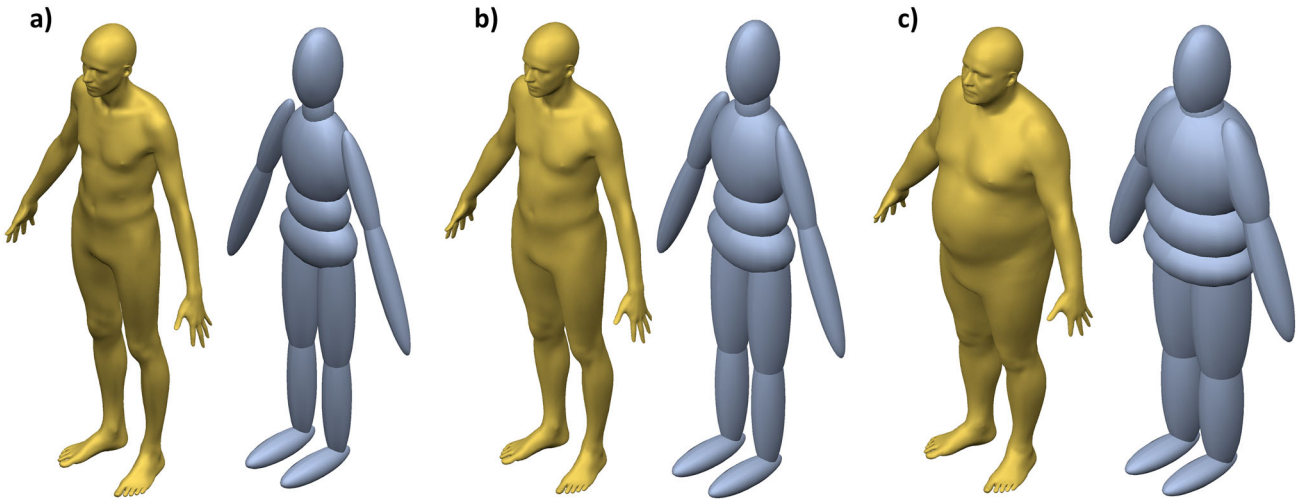

Fig. 3 Example of sample subjects: **a** under-weight subject (#2); **b** normal-weight subject (#9); **c** obese subject (#19)

($\sigma^2_{A-Actual}$); the number of degrees of freedom was calculated as the number of subjects in the datasets multiplied for the number of nodes, so in this test the degrees of freedom were set equal to infinite for both σ^2_{E-A} and $\sigma^2_{A-Actual}$.

Other statistical tests were performed to assess the relevance of differences between the two models calculated over all subjects. A paired-samples Wilcoxon test was used to analyze the inertial parameters, and an F-test was conducted to examine the geometry deviations. The significance level for both analyses was set at 0.01.

2.4.3 Principal moments of inertia and masses analysis

A linear regression analysis was performed where the ellipsoids model's properties are reported versus the anthropomorphic model's properties; considering, for example, the mass property:

$$Mass_{E,s,b} = f\left(Mass_{A,s,b}\right) \tag{8}$$

Regression line parameters (slope m and offset q) and correlation coefficient R were computed. This regression would be close to a line with unitary slope and passing through the axes origin if the ellipsoids model was able to provide an unbiased estimate.

In addition, absolute (ε_{abs}) and relative (ε_{rel}) errors analyses were performed for inertial parameters; considering again the mass property as an example, the absolute error was computed as:

$$\epsilon_{abs,M,s,b} = \Delta M_{s,b} = M_{E,s,b} - M_{A,s,b} \tag{9}$$

The $\varepsilon_{abs,Mass,s,b}$ error was evaluated for all 20 subjects and for all 15 body segments; then, for each segment b, the mean value $\mu_{\varepsilon,abs,M,b}$ and the standard deviation $\sigma_{\varepsilon,abs,M,b}$ of this error were computed over all subjects.

The mean relative error $\mu_{\varepsilon,rel,M,b}$ was evaluated as:

$$\mu_{\epsilon,rel,M,b} = \frac{\mu_{\epsilon,abs,M,b}}{\mu_{A,Mass,b}} \times 100 \tag{10}$$

where $\mu_{A,Mass,b}$ is the mean value for the anthropomorphic-based parameters.

2.4.4 Centre of mass and joint centre locations analysis

All 3D models were centred on the abdomen centre of mass (approximating the whole-body G parameter [17, 27]) and the deviation between the ellipsoids and anthropomorphic ATB model in terms of centres of mass (G) and joints centre (J) locations were assessed. From a preliminary analysis the error along the vertical direction (z axis in Fig. 4) has resulted to be less affected by slight posture's variations, compared to the x and y components; therefore, only the $G_{z,m,s,b}$ and $J_{z,m,s,j}$ components have been analysed in the following:

$$\epsilon_{abs,G,z,s,b} = G_{z,E,s,b} - G_{z,A,s,b} \tag{11}$$

$$\epsilon_{abs,J,z,s,b} = J_{z,E,s,j} - G_{z,A,s,j} \tag{12}$$

Moreover, arms were properly oriented in order to minimize the position error with reference to the anthropomorphic model (Fig. 4).

2.4.5 Multibody simulation analysis

A fall from 6 m height was simulated for subject 7 (obese sample), whose multi-ellipsoidal model appeared to be the most different from the corresponding anthropomorphic ATB model. Two different scenarios were created in the multibody code considering a fall from a balcony and a fall without midway impacts (Fig. 5a, b), in order to differentiate the relevance of inertial and geometrical factors on numerical results.

These simulations were performed under the same boundary conditions (subject's initial velocity, model constraints, contact parameters). An initial linear velocity along the y axis was imposed to the thorax segment centre of mass (v_i= 4 m/s) to simulate an external pushing force, acting on the subject.

The anatomical joints in both ATB models were modelled in the same manner (revolute or spherical joints) and they were assigned the same passive properties, based on a previous work by some of the authors [35]. It is important to stress that both ATB models were passive models, meaning that no muscle activation was modelled. This aspect, added to the external pushing action simulated as an initial condition, allows to reproduce an unconscious body falling. Contact laws for segment-to-segment or for segment-to-environment were modelled considering formulations available in Adams and the stiffness and damping properties listed in Online Resource 2 were implemented.

Contact and friction parameters were selected (Online Resource 2) avoiding high body-to-body penetrations (< 10 mm) and preventing sliding of the body on the ground.

3 Results

3.1 3D External Geometry

F-test analysis has testified that the variance observed between the ellipsoid model and the anthropomorphic geometry is significantly higher than the variance observed between the anthropomorphic geometry and the actual body

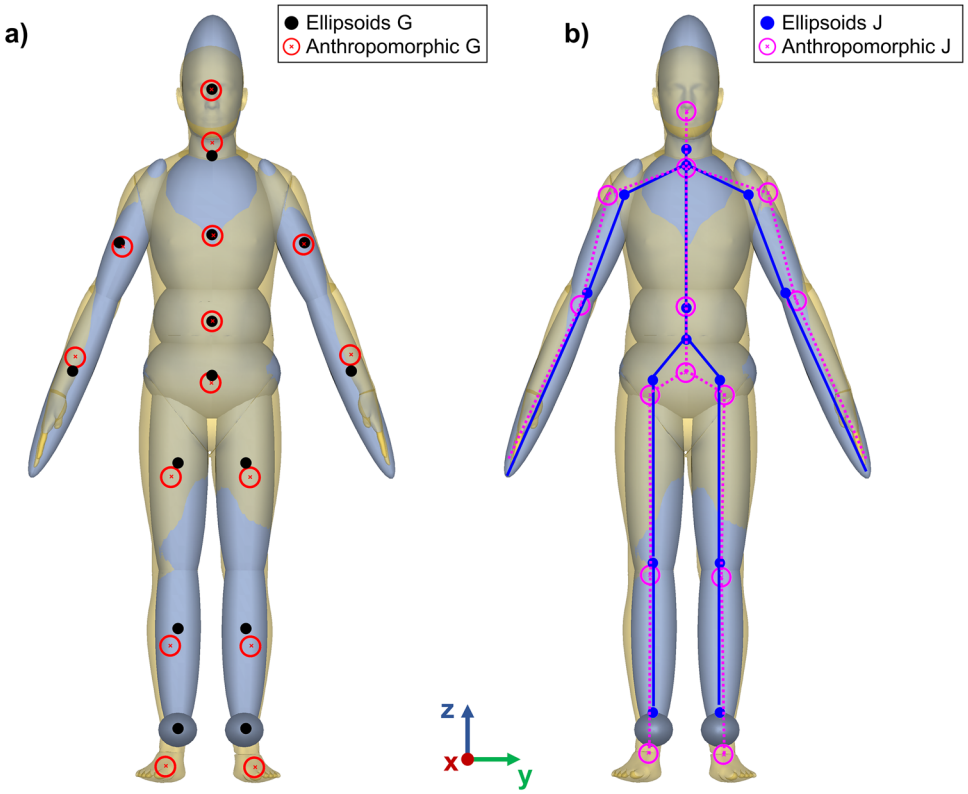

Fig. 4 **a** Centres of mass location and **b** joints centres locations comparison

shape (54.6 versus 5.06 mm^2, $p < 0.01$). According to this result, the anthropomorphic model will be used as a reference in the following analyses.

The error distribution for the 3D external geometry is graphically represented by a box plot in Fig. 6a. For each subject the 10-th and 90-th percentile values are represented by the boxes' boundaries, while the ends of the whiskers (black dashed lines) correspond to the maximum and minimum values of the geometrical error; red lines and red squares show the median and average error, respectively. The mean error resulted to be consistent among all 20 subjects, with an average value equal to 23 mm, while a deviation of 50 mm is exceeded by 10% nodes. An example of the geometrical error distribution is shown in Fig. 6b for a sample subject (Subject 16, over-weight); generally speaking, the most critical areas are represented by shoulders, arms and calves (orange and red areas in Fig. 6b). For over-weight subjects the maximum error rose up to 130 mm and it was located at the trunk region.

3.2 Principal Moments of Inertia and Mass

Linear regression analysis results for the mass property are reported in Fig. 7. The same general trend was observed among all inertial properties (for complete results the reader can refer to online resource 3): when considering data from all segments, a strong correlation index was found (> 0.95) and the regression line exhibited a slope close to unity and intersected with the origin. According to this evidence, the ellipsoids model provided a very good approximation of inertial properties calculated from the actual geometry (Fig. 7 left).

However, the regression model was not able to provide an equally good approximation for all segments, as evident when data values are analysed segment by segment. Indeed, the thorax, thighs, upper arms and calves inertias are overestimated, lying systematically above the regression line; conversely, data associated to the abdomen, pelvis and neck segments are underestimated, being below the line.

The absolute error analysis confirmed the results of the regression analysis for what concerns the trend of specific segments (Fig. 8). Looking at relative errors (Online Resource 4), the abdomen segment was the most critical with reference to both principal moments and mass parameters, having observed a mean relative error equal to about 65% and 60% respectively. Along with the abdomen, also the upper arms exhibited mean error values equal to approximately 30% for the mass and 63% for the principal moments.

As a general rule, the mass estimates provided by the multi-ellipsoidal model resulted to be more accurate compared to principal moments of inertia's estimates.

The significance analysis has revealed that there were notable differences between the ellipsoidal and anthropomorphic models across all segments, exception made for the thorax I_{zz} value and for the head mass (Fig. 8a, b).

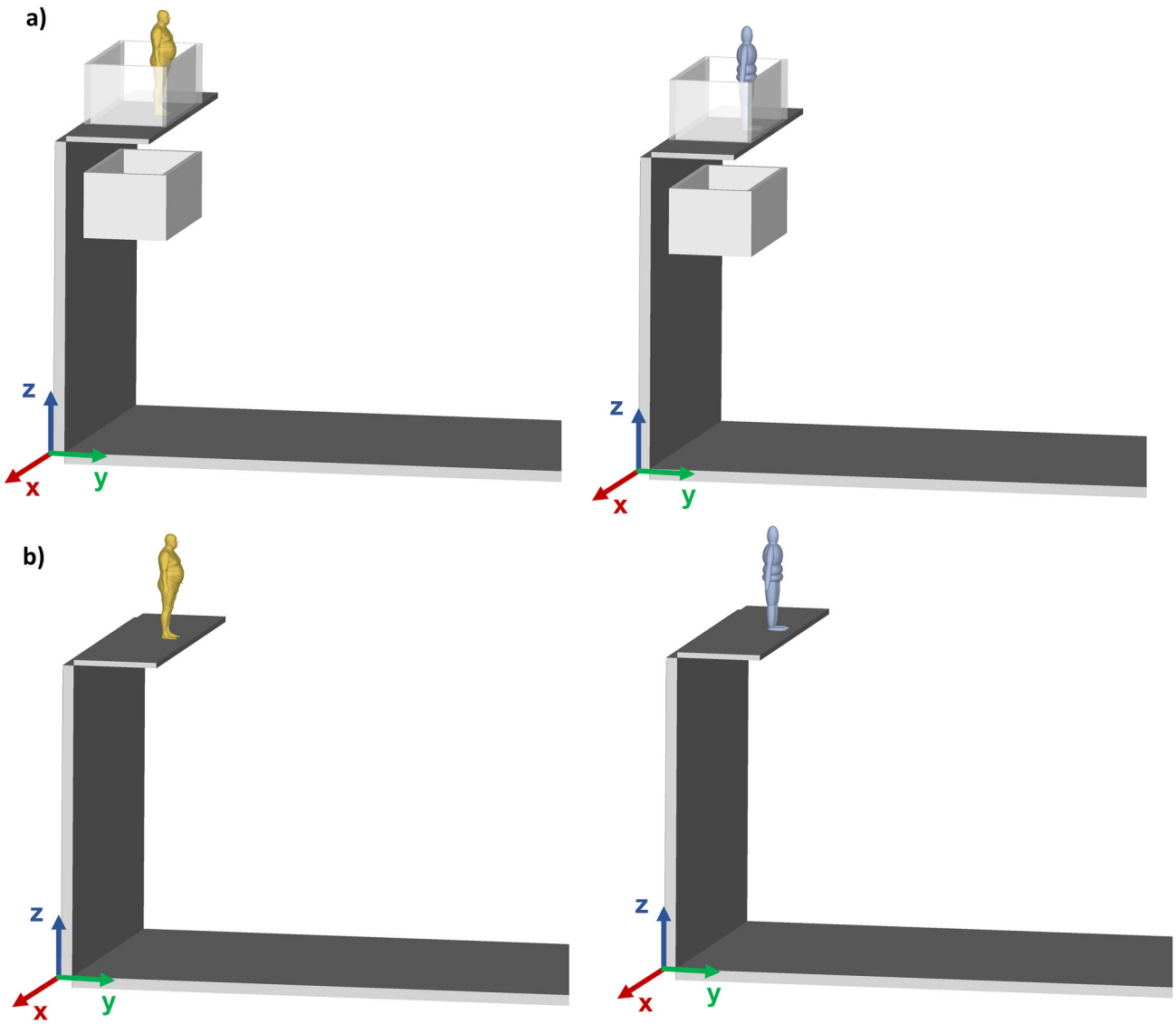

Fig. 5 Multibody models initial configurations: **a** fall from a balcony; **b** fall without midway impacts

3.3 Centre of Mass and Joint Centre Location

Many critical segments were identified with reference to the position of centres of mass and joints. Figure 9a, b show errors along the z direction (average value and standard deviation).

As the centres' distance from the abdomen increases, errors tended to cumulate. An additional analysis was therefore performed to better understand the contribution of each segment, making use of a variable reference frame, that is the centre of mass of the next segment moving from the head to the feet (refer to Online Resource 5): for example, the head-neck error represents the head centre of mass error with respect to the neck centre of mass location. With this new representation, the head, neck, forearms and thighs were the most critical segments for what concerns the centre of mass location.

According to Wilcoxon test, only the right forearm centre of mass location G_z was not significantly different between the multi-ellipsoids and the anthropomorphic model (Fig. 9a, b).

3.4 Multibody Simulation Analysis Results

The multibody simulation pointed out relevant differences between the multi-ellipsoids and the anthropomorphic models when the fall from a balcony scenario is considered. First of all, the sequence of contacts between the subject and the respective environment (the balcony and the ground) is different (Fig. 10a, b) as well as impact forces magnitude (and the resulting injury) (Fig. 11). These differences are due to the

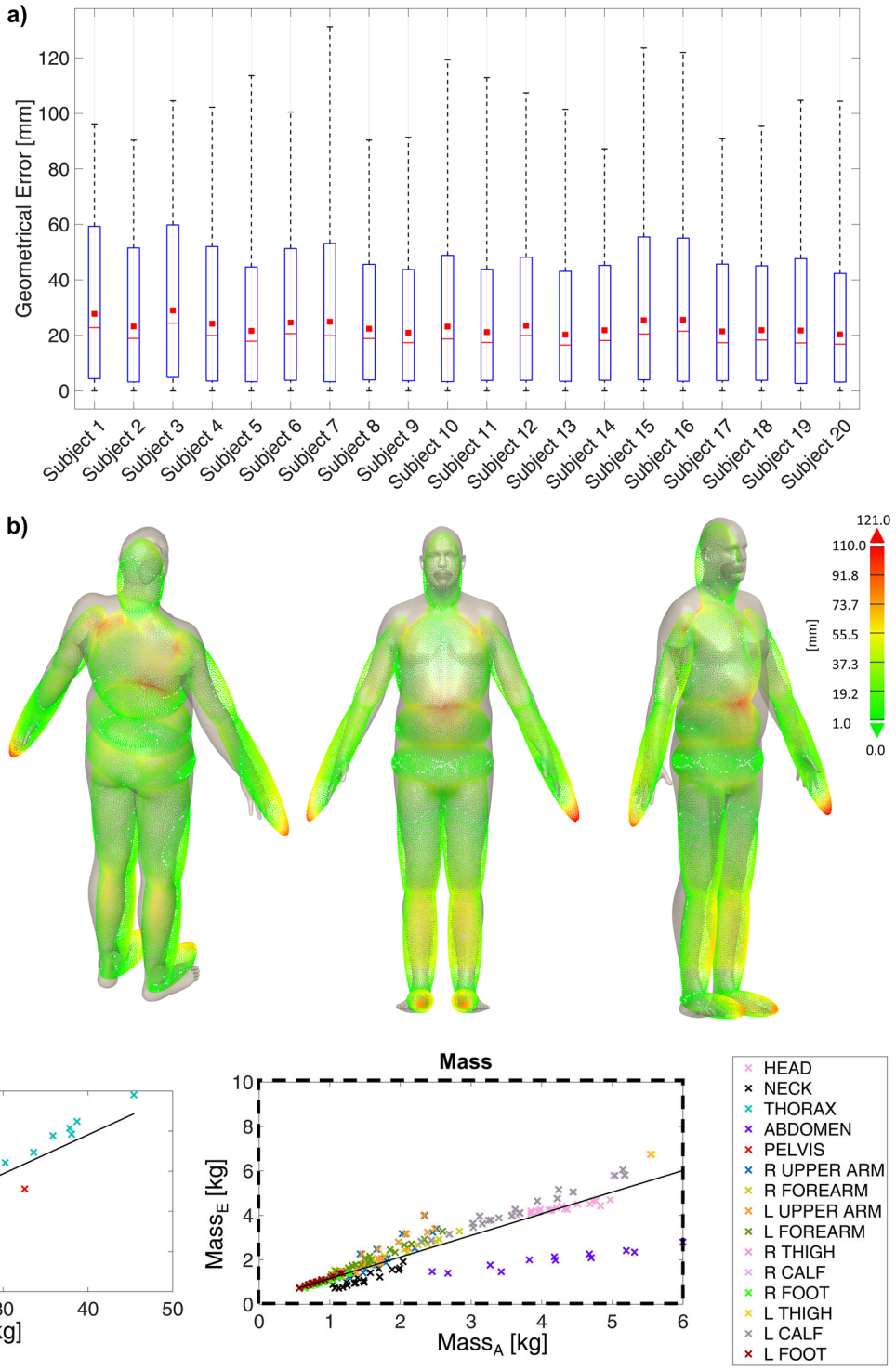

Fig. 6 Geometrical error analysis: **a** box plot representation of 10-th and 90-th percentile (blue boxes boundaries), maximum and minimum errors (whiskers), median (red lines), average error (red squares); **b** geometrical error distribution for an over-weight subject

Fig. 7 Regression analysis results for the mass parameter. Left: full data representation; right: detail of near-to-origin data. Here only data for the mass are reported; a complete representation of regression analysis for all inertial properties can be found in Online Resource 3

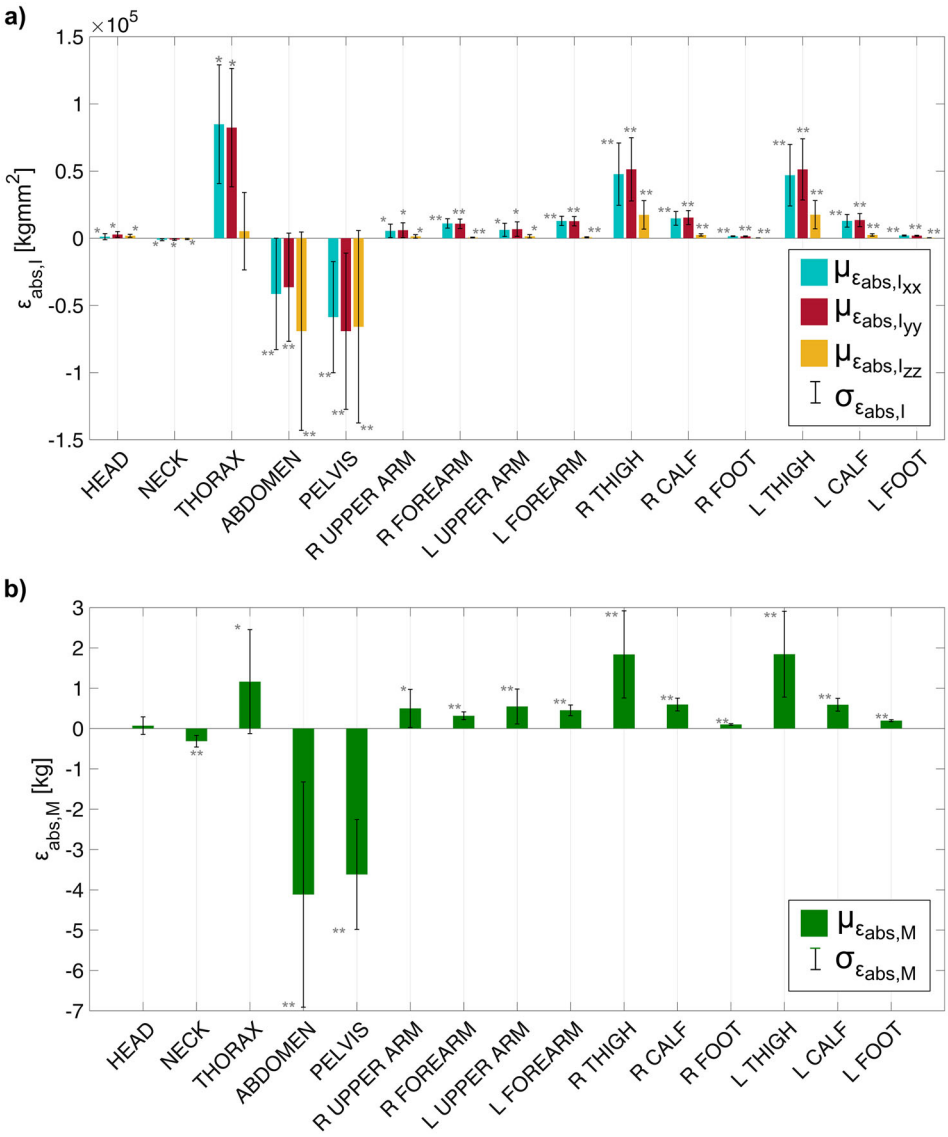

Fig. 8 Absolute error distribution for inertial parameters: **a** principal moments of inertia; **b** mass. *($p < 0.05$) and **($p < 0.0001$) indicate significant differences between the ellipsoids and the anthropomorphic reference model

interactions between body segments and the external environment and lead to a different kinematic throughout the fall and a different final configuration (Fig. 10a). In fact, differences between the two models were partly due to differences of inertial moments, and partly to differences of the external geometry. The second factor has a greater impact when multiple contacts take place as in the present case. Following body rotation around the balcony, the trajectories of the center of mass (Fig. 10b) exhibited significant differences, as demonstrated by the final rotation angles about the y axis for the head and the hips: this value was close to 270° in the ellipsoids model while it was greater than 360° for the anthropomorphic model, in fact the anthropomorphic ATB model performs a full rotation during its fall.

If the analysis is repeated under the same initial conditions but in an 'open' space; results depicted in Figs. 12 and 13 are obtained. As can be seen, differences between trajectories get smaller and the kinematics followed a more similar pattern in terms of both body's centre of mass trajectories and body rotations.

4 Discussion

This study was aimed to present a new methodology for the creation of an anthropomorphic ATB model for multibody analyses, and to investigate differences, in terms of geometrical and inertial segments' properties, of ellipsoids-based models. In particular, the GEBOD program was chosen for the prediction of the ellipsoidal ATB model, having considered that, over the years, this was one of the most used datasets and moreover, its documentation is fully accessible and can be easily implemented.

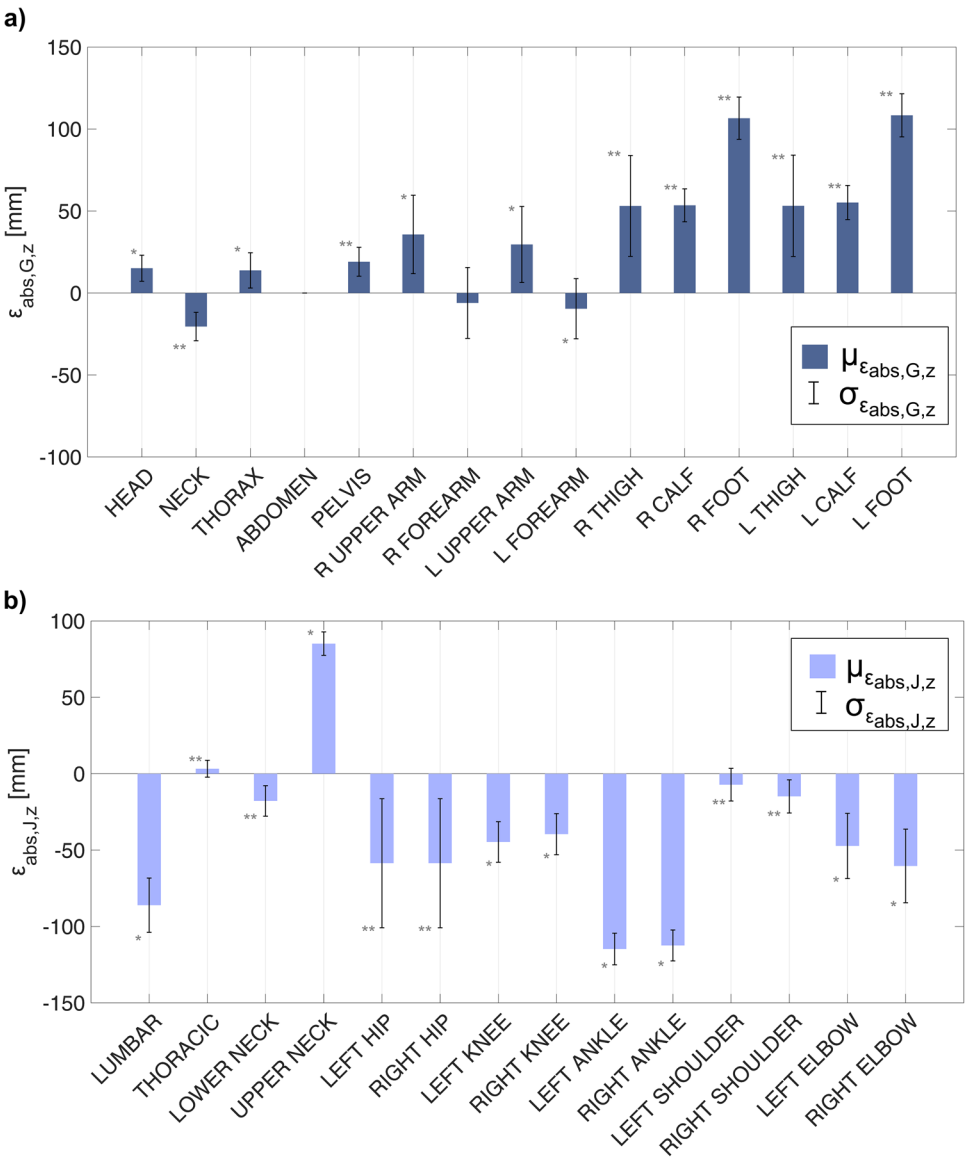

Fig. 9 Mean and standard deviation of the absolute error in vertical direction for **a** centres of mass and **b** joints' centres location. *($p < 0.05$) and **($p < 0.0001$) indicate significant differences between the ellipsoids model data and the anthropomorphic reference model

Various works in literature are aimed to establish new procedures for a more accurate estimation of body parameters, using both indirect estimation from surface data reconstruction (i.e., laser scanning) [29, 32] and direct measurements from radiation-based methods (such as X-ray, DEXA, CT scans) [1, 2] or experimental tests [54]. These studies have been focused either on some specific body segments or on whole-body inertial properties, and have considered various properties among geometrical, inertial, and so on. Schultz et al. [54] have directly measured whole-body inertial properties of 69 volunteers (34 females and 35 males) and compared results with values calculated using the GEBOD program. More recently, Durkin et al. [1] and Merril et al. [2] have used DEXA to predict body segment parameters and evaluate the prediction ability with respect to literature data [12, 14, 55]: Durkin focused on the lower leg (calf) and proposed an elliptical model based on density distribution data; Merril considered the torso, thigh, lower leg, upper arm and forearm segments comparing DEXA results with literature data and obtaining a prediction error of about 5% of the actual DEXA-based values, against errors up to 60% for the de Leva regressions. 3D photogrammetry was used by Peyer et al. [32] for obtaining the full-body surface of four male subjects, evaluating inertial properties of the thigh and shank segments and comparing results with regression models [6, 12]. A similar approach was followed by Smith et al. [29], who have proposed a subject-specific body segmentation based on full-body scans of 95 males and females volunteers and compared segment properties computed from this segmentation to cadaveric data [6, 12–14]. Having considered promising results obtained by Smith et al. [29] in the application of laser-scan technique, this study was aimed to

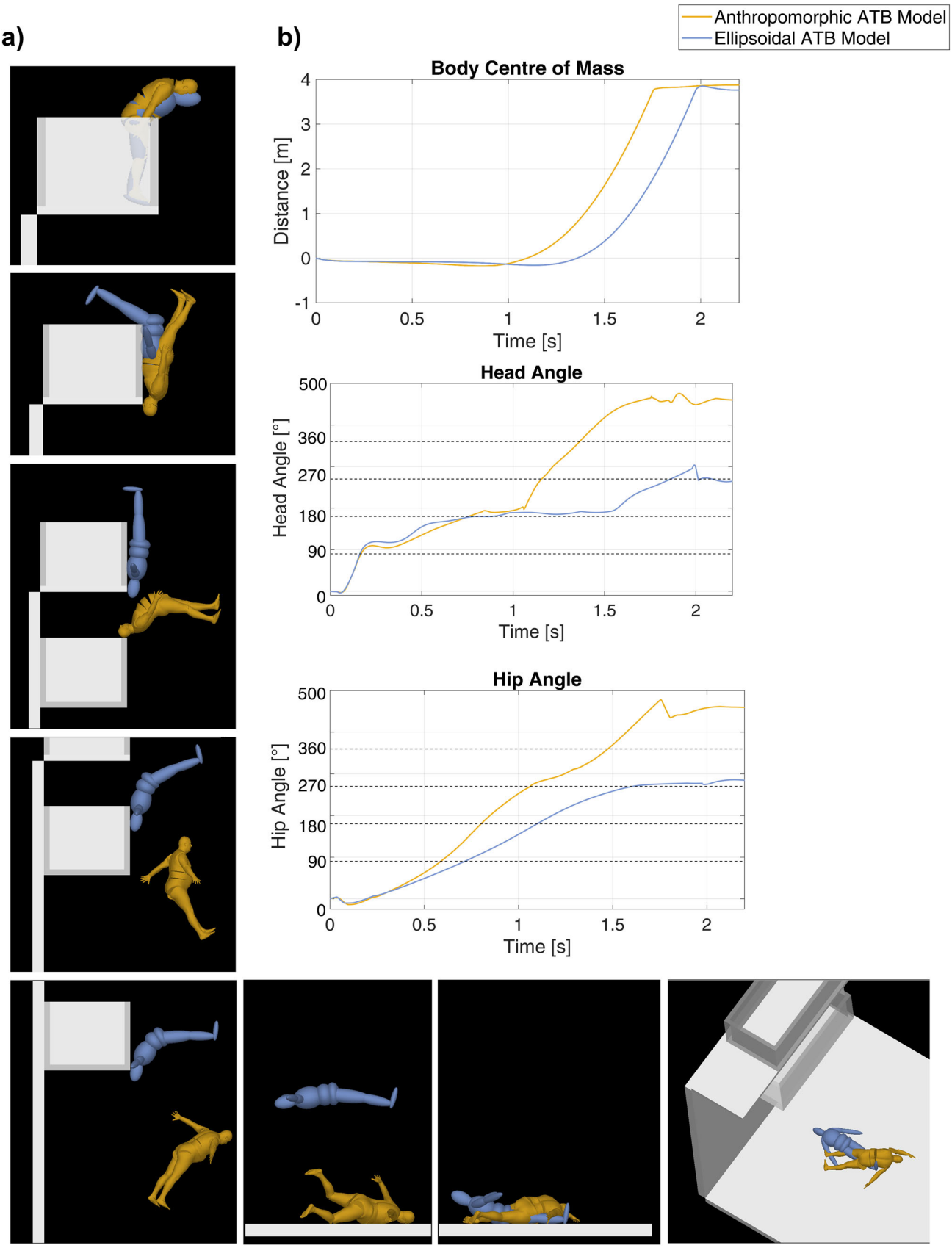

Fig. 10 **a** Global kinematic of the fall from a balcony; **b** centre of mass trajectory, head and hip rotation angles throughout the falling motion (dashed black lines represent rotation angles of 90°, 180°, 270°, 360°)

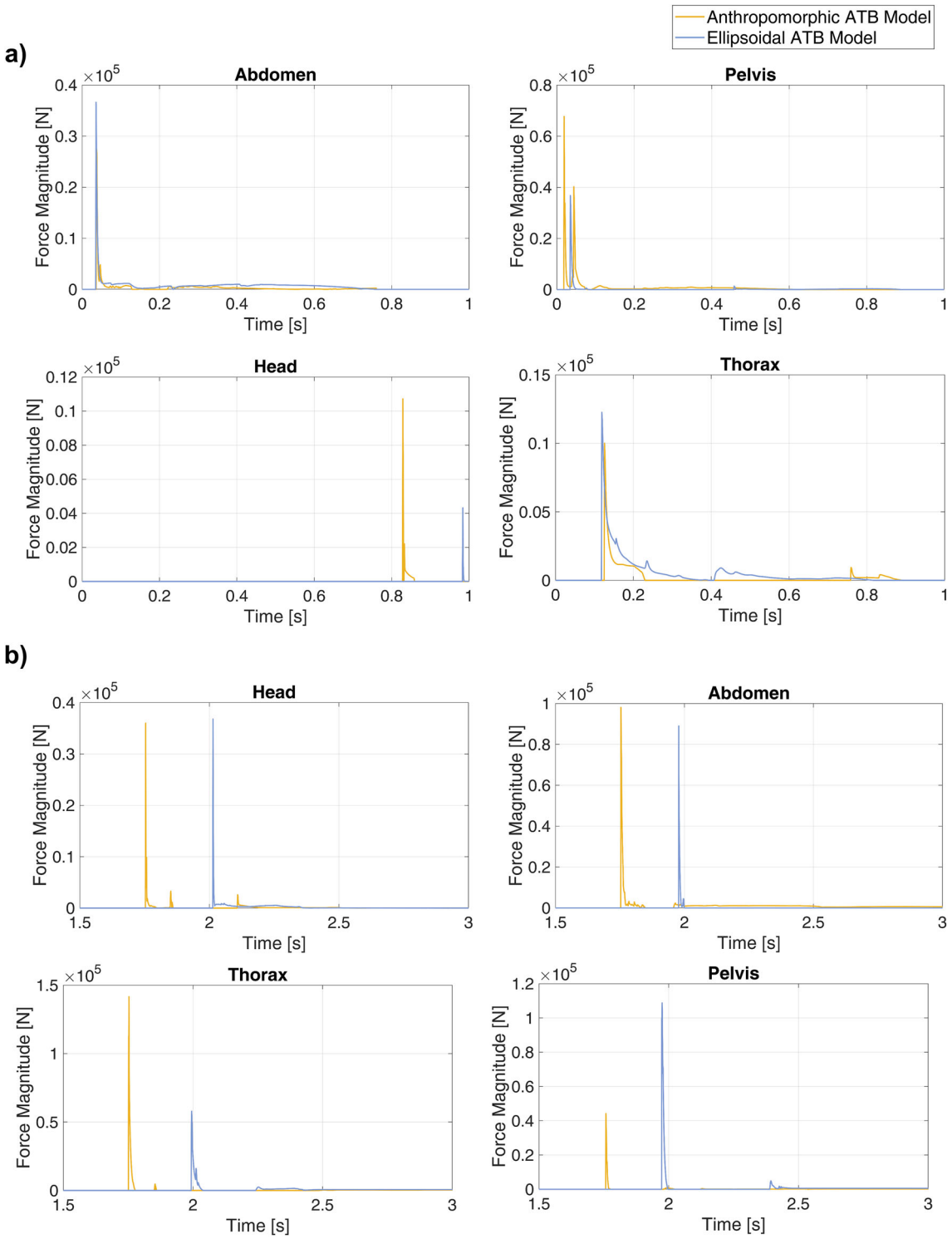

Fig. 11 Contact forces magnitude for head and trunk segments with the balcony (**a**) and the ground (**b**)

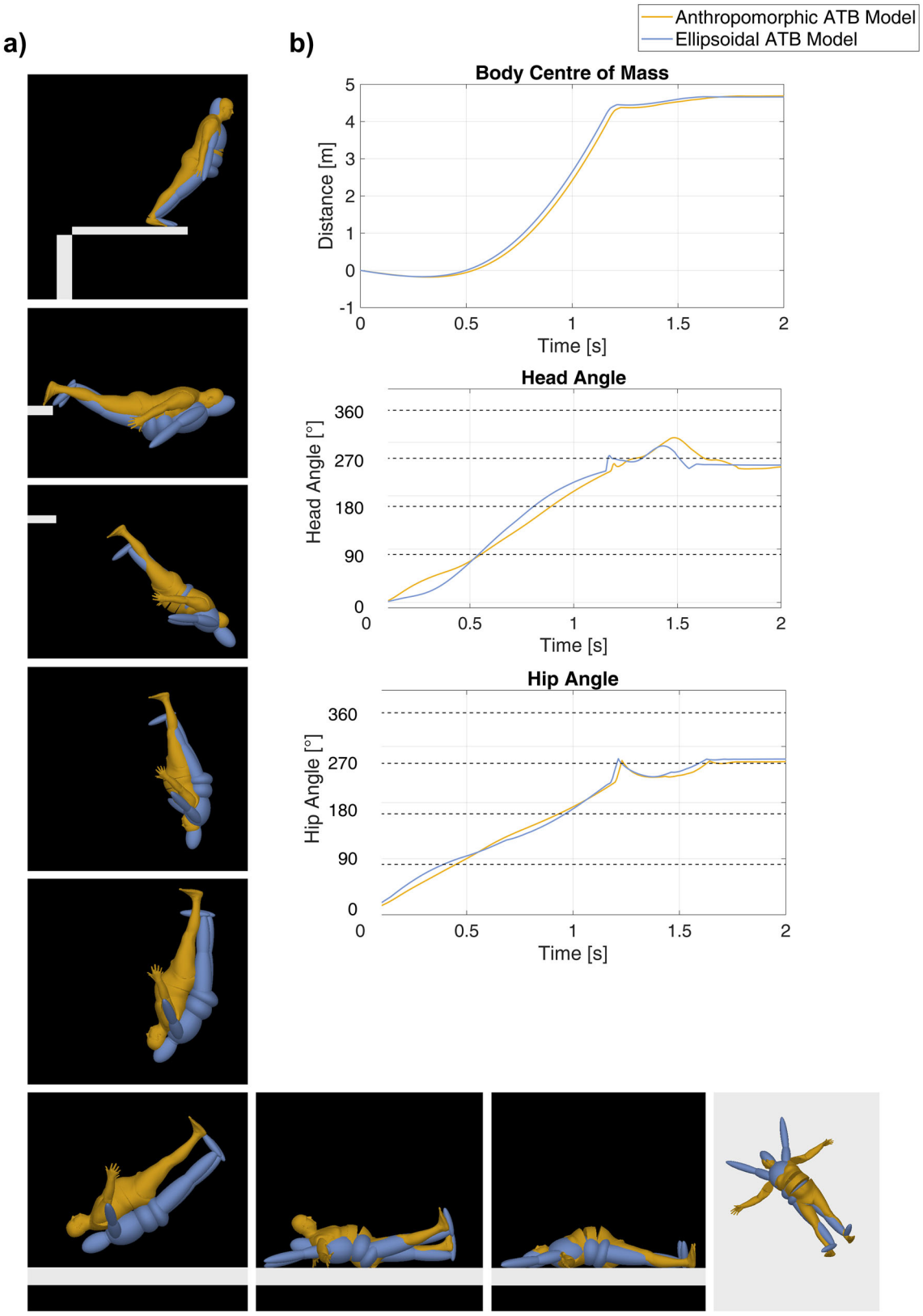

Fig. 12 **a** Global kinematic of the fall without midway impacts; **b** centre of mass trajectory, head and hip rotation angle throughout the falling motion (dashed black lines represent rotation angles of 90°, 180°, 270°, 360°)

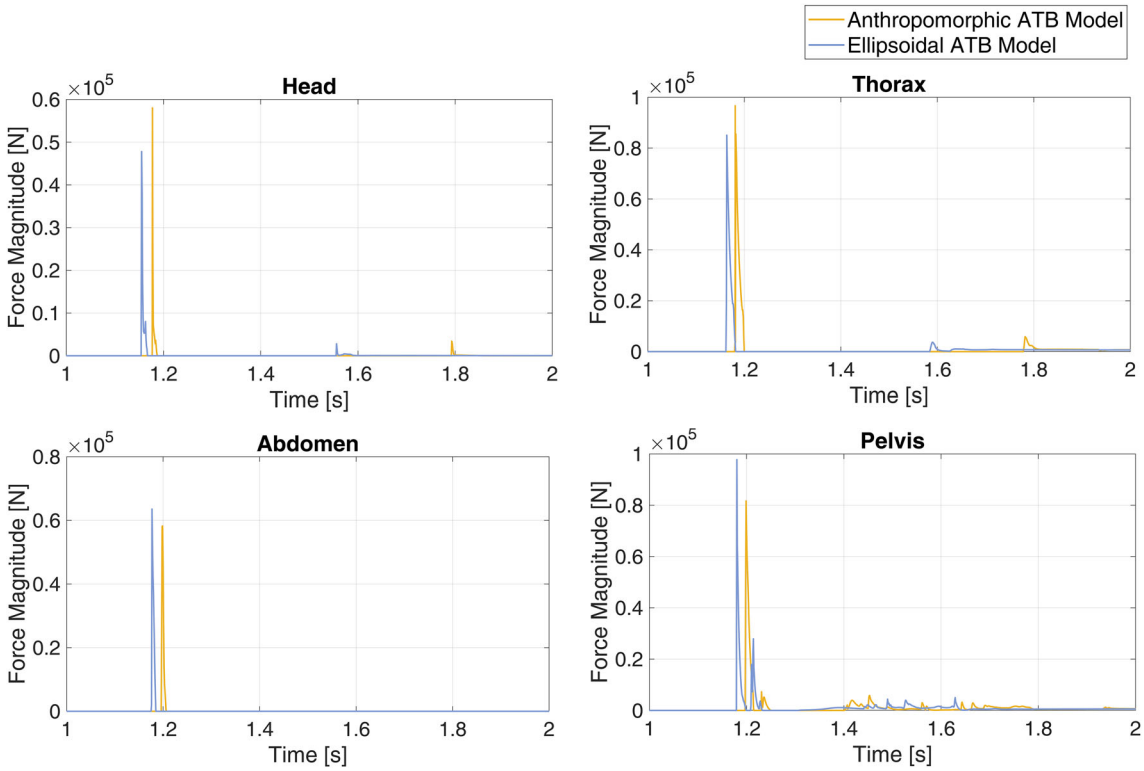

Fig. 13 Contact forces magnitude between head and trunk segments and the ground

provide a more accurate and less time consuming procedure for the human body geometry creation based on a database of over a thousand 3D scans (CAESAR database) and on the application of SSM, leading to an anthropomorphic model. The accuracy of geometric reconstruction was assessed in a previous work [33], and it was here demonstrated to be significantly higher compared to the accuracy of ellipsoids models. The performance of the classical ellipsoids model was then tested against this new methodology, considering all parameters which might be influential on multibody analyses: the geometry, the inertial properties, the joint locations. Some significant differences have been found, as detailed in the following. In terms of body mass, the abdomen was identified as the most critical segment, with a relative error of approximately 60%; this segment remains critical also for the principal moments of inertia (65% error), confirming the underestimation of its inertial properties by the ellipsoids model. Also the upper arm segments were found to be affected by a high error in principal moments of inertia, with a 63% overestimation. In the sample set being analyzed, it is noteworthy that the maximum errors are primarily associated with individuals who are either obese or underweight. This outcome is not surprising, given that the ellipsoids-based properties were calculated over a population that did not includes such individuals.

For what concerns the centre of mass location, the absolute error analysis has shown that the most critical segments exhibited mean errors between 35.7 and 53.5 mm, while only the feet have errors above 100 mm.

In addition, differences between predictions obtained by the two models were found to be significant for all the inertial properties, ($p < 0.0001$), exception made for the thorax I_{zz} and the head mass (5.25×10^3 kg mm^2 and 0.0715 kg absolute error respectively).

In previous works, deviations between computed inertial parameters and cadavers' studies were compared, and the results were consistent with the findings of our current research.

The 3D scanning method proposed in the work by Smith et al. [29] pointed out significant errors in the estimation of the masses of feet, upper arms and head. These segments were found to be critical also in our analyses, but with higher relative error values (below 10% in Smith et al. [29]). Smith did not reveal any criticism for trunk's segments, while these segments have exhibited the highest deviations in the present study, especially the abdomen; these differences can be related to the different populations involved in the two studies (Smith et al. work did not consider under- and overweight subjects) and to the fact that in [29] the trunk was not segmented in three different parts but it was considered

a unique body from the neck base to the hips. With reference to the centre of mass location, Smith found that thighs, forearms, calves and upper arms deviate by 10–25% from literature data, while the multi-ellipsoids and anthropomorphic models have shown higher errors for the forearms and thighs segments (41 mm and 34 mm respectively). Finally, Smith et al. compared principal moments of inertia not only against cadaver data, but also with stereophotometric data reported by McConville [17], that are the same data implemented in the GEBOD model: from this comparison, results similar to those presented in the present study can be found, having identified high deviations for the thigh and calf segments, whose principal moments are overestimated by the regression model. Furthermore, also the 3D scanning results presented by Peyer et al. [32] have highlighted that the thighs are very critical for inertial properties estimation, and results coming from DEXA [2] analysis have assessed that thighs and torso parameters definition needs to be improved, due to significant errors usually associated to these segments. From these findings, a general agreement with similar studies has emerged, having identified the same critical segments deserving further inquiries with reference to inertial body properties. Furthermore, the present study addressed the limitations associated with the 3D scanning process (removal of hair from the head segment and loss of the inferior part of the feet) thanks to the high accuracy of CAESAR database.

Looking at geometrical analyses, results have shown that the multi-ellipsoids model geometry has a significant deviation from the anthropomorphic one, with errors getting higher as the subject's morphology deviates more significantly from the normal-weight: distances between the actual geometry and ellipsoids geometry can reach 130 mm for more obese patients, while it usually keeps below 50 mm.

These differences have been proved to have a relevant impact on ATB models implemented in multibody simulations.

Regarding the simulation of free fall, both kinematic (Fig. 12b) and impact forces (Fig. 13) are comparable between the two models. These findings can be roughly validated by examining the trajectory of a single mass concentrated in the centre of mass of the body and comparing them with analytical and experimental [56–58] data. Additionally, more refined validation of the ellipsoid model has been conducted in the past, which considered 50-th and 95-th percentile subjects, and their kinematic and dynamic response after an impact in confined spaces [59–64]. The good correspondence found between the anthropomorphic model and the ellipsoidal one in a simple free fall condition further validates the output of the anthropomorphic model, as expected given its higher accuracy in geometry reconstruction.

The anthropomorphic model's power lies in its ability to predict impact with other bodies more accurately due to its precise definition of the outer body geometry. Furthermore, it provides a more consistent performance with reference to 'out of standard' morphologies, such as obese or underweight subjects. This is due to the regression equation used for the estimation of ellipsoids properties, which were obtained with a limited number of inputs (height, weight, and gender) and through minimization of the sum of squares, meaning that subjects who are more represented (i.e., within the 95-th percentile) are better fit.

When a fall from a height occurs with midway impacts, such as in the balcony simulation presented here, there are differences in both the global kinematics and dynamics of impacts with the surrounding environment. Since models have provided similar and reliable results for free falls, the deviations between the two models have to be attributed to the different interaction of body segments with the environment (balcony). At the beginning of the simulation, before the interaction with the balcony geometry, the kinematics of the two models are similar (Fig. 10a). In the next step, the anthropomorphic ATB model experiences a major first impact with the balcony at the pelvis level (Fig. 11a), while the ellipsoidal model undergoes a significant impact at the abdomen segment level and this is due to significant differences in solid models used to reproduce trunk geometries, especially with reference to the pelvis.

After the first impact, the thorax and abdomen segments come into contact with the balcony rail in the multi-ellipsoid model, and the model is actually entangled due to residual spaces between ellipsoids. This leads to a longer interaction with the balcony compared to the anthropomorphic model, which interacts with the balcony mainly at the level of the pelvis segment. In the following steps, the entanglement between the tights and pelvis of the multi-ellipsoid model plays a major role in determining the rotation of the legs over the balcony rail. Compared to the anthropomorphic model, the ellipsoidal one shows a delay in leg rotation, which ultimately results in a closer contact to the balcony outer surface. The differences above described produced a different final position on the ground at the end of simulation.

An important aspect outlined by these numerical analyses was that simulation times did not exhibit consistent differences between the two models (about 5 s on a computer with i7-8700 CPU and 32 GB RAM), maintaining the same low computational effort typically associated with ATB models.

The comparison analysis between the anthropomorphic and the GEBOD models here presented is certainly affected by some limitations. First of all, the segmentation process here proposed is based on the individuation of anatomical skin landmarks, which implies that resulting limbs segments are not perfectly symmetrical between the left and right sides; on the contrary, the GEBOD program generates datasets that are symmetrical, meaning that the same geometrical and inertial properties are assigned to right and left limbs segments.

In the second place, the segmentation process itself can have an influence on data comparison: landmarks identified in the current study might be slightly different from those identified over 30 years ago, with less advanced techniques. In addition, a 'standardised' subdivision of the human body in segments still does not exist, and this makes impossible the comparison between the findings of this work and other works in literature.

5 Conclusions

In this work a methodology for the creation of an anthropomorphic external geometry of a human subject was presented, with the aim of investigating body segments properties taking one step further with respect to existing studies. The 3D geometry generation was based on a Statistical Shape Model, built from a wide database of 3D human scans (CAESAR database) and implemented into a code developed for ergonomic design studies [43], here extended to be implemented in a multibody code (MSC Adams). A virtual population made of twenty adult males was selected as a subset for this study and anthropomorphic and multi-ellipsoidal models were created for each individual. The first objective of the present work was to compare the main properties of body segments (inertial properties, joint centres positions, external geometries) between the two modelling approaches. The analysis has pointed out how the abdomen and the thighs are the most critical segments with reference to inertial properties, while the most critical areas, for what concerns the external geometry, are located at the shoulders, the calves, and, for over-weight and obese subjects, at the trunk. These differences can have a significant impact on the outcome of multibody analyses: a reference case of a human falling from a balcony has been here analysed; the contact sequence has resulted to be different between the two models as well as the peak impact forces. On the whole, the anthropomorphic model represents an advancement towards a more faithful simulation of the human body behaviour, thanks to an accurate reproduction of its external shape. In order to improve the anthropomorphic ATB model, future activities will be focused on overcoming limitations related to the segmentation of the human body geometry. One of the consequences of this segmentation process is that segments' geometries have sharp edges at the end surfaces, differently from rounded structures of ellipsoids. When relative rotations between segments are relevant, these sharp corners can generate some gaps, which can be unsightly and can affect simulation results when contacts taking place next to those areas are of relevance. To address this issue, anthropomorphic ATB models including flexible elements between adjacent body segments will be investigated in the future.

Supplementary Information The online version contains supplementary material available at https://doi.org/10.1007/s12008-023-01427-0.

Acknowledgements This work was supported by Grants "Ricerca di base 2020" from Università degli Studi di Perugia.

Funding Open access funding provided by Università degli Studi di Perugia within the CRUI-CARE Agreement.

Declarations

Conflict of interest The authors declare that they have no conflict of interest. The author declares not to have any financial or non-financial interests directly or indirectly related to this work.

References

1. Durkin, J.L., Dowling, J.J.: Body segment parameter estimation of the human lower leg using an elliptical model with validation from DEXA. Ann. Biomed. Eng. **34**, 1483–1493 (2006). https://doi.org/10.1007/s10439-006-9088-6
2. Merrill, Z., Perera, S., Cham, R.: Predictive regression modeling of body segment parameters using individual-based anthropometric measurements. J. Biomech. **96**, 109349 (2019). https://doi.org/10.1016/j.jbiomech.2019.109349
3. Shand, S.: Pedestrian whole body ground contact mechanisms and head. Injury Assessment Following Vehicle Impact (2020)
4. Haug, E., Choi, H.Y., Robin, S., Beaugonin, M.: Human models for crash and impact simulation. Handb. Numer. Anal. **12**, 231–452 (2004). https://doi.org/10.1016/S1570-8659(03)12004-2
5. Pearsall, D.J., Reid, J.G.: The study of human body segment parameters in biomechanics. Sport Med. **18**, 126–140 (1994). https://doi.org/10.2165/00007256-199418020-00005
6. Clauser, C.E., Mcconville, J.T., Young, J.W.: Weight, Volume, and Center of mass of segments of the human body (1969)
7. Hertzberg, H.T.E., Dupertuis, C.W., Emanuel, I.: Stereophotogrammetry as an Anthropometric Tool. Wright Air Development Center, Air Research and Development Command, United States Air Force (1958)
8. Cavanagh, P.R., Gregor, R.J.: The quick-release method for estimating the moment of inertia of the shank and foot. In: Nelson, R.C., Morehouse, C.A. (eds.) Biomechanics IV: Proceedings of the Fourth International Seminar on Biomechanics, University Park, Pennsylvania. Macmillan Education UK, London, pp. 524–530 (1974)
9. Rossi, M.M., Alderson, J., El-Sallam, A., et al.: A new validation technique for estimations of body segment inertia tensors: principal

axes of inertia do matter. J. Biomech. **49**, 4119–4123 (2016). https://doi.org/10.1016/j.jbiomech.2016.10.006
10. Harless, E.: The static moments of the component masses of the human body. Trans. Math-Phys. Royal Bavarian Acad. Sci. **8**(l), 69–96 (1860)
11. Maquet, P.G.J., Braune, W., Furlong, R., Fischer, O.: On the centre of gravity of the human body: as related to the equipment of the german infantry soldier. Springer, Berlin (2012)
12. Dempster, W.T.: Space requirements of the seated operator: geometrical kinematic and mechanical bspects of the Body with special reference to the limbs. Wright-Patterson AFB Ohio, Wright Air Development Center (1955)
13. Chandler, R. F.; Clauser, C. E.; McConville, J. T.; Reynolds, H. M.; Young, J. W.: Investigation of Inertial Properties of the Human Body. Air Force Aerospace Medical Research Laboratory; Wright-Patterson AFB, Ohio (1975)
14. de Leva, P.: Adjustments to Zatsiorsky–Seluyanov's segment inertia parameters. J. Biomech. **29**, 1223–1230 (1996). https://doi.org/10.1016/0021-9290(95)00178-6
15. Jensen, R.K., Fletcher, P.: Distribution of mass to the segments of elderly males and females. J. Biomech. **27**, 89–96 (1994). https://doi.org/10.1016/0021-9290(94)90035-3
16. Durkin, J.L., Dowling, J.J.: Analysis of body segment parameter differences between four human populations and the estimation errors of four Popular Mathematical Models. J. Biomech. Eng. **125**, 515–522 (2003). https://doi.org/10.1115/1.1590359
17. Mcconville, J.T., Churchill, T.: Anthropometric relationships of body and body segment moments of Inertia. Report. **105**, 7405–7409 (1980). https://doi.org/10.1073/pnas.0710346105
18. Damavandi, M., Farahpour, N., Allard, P.: Determination of body segment masses and centers of mass using a force plate method in individuals of different morphology. Med. Eng. Phys. **31**, 1187–1194 (2009). https://doi.org/10.1016/j.medengphy.2009.07.015
19. Chambers, A.J., Sukits, A.L., McCrory, J.L., Cham, R.: The effect of obesity and gender on body segment parameters in older adults. Clin. Biomech. **25**, 131–136 (2010). https://doi.org/10.1016/j.clinbiomech.2009.10.015
20. Rout, B., Dash, R., Dhupal, D., Das, S.R.: Optimized posture prediction for task specific during stacking process using human upper body movements. Int. J. Interact. Des. Manuf. **16**, 291–303 (2022). https://doi.org/10.1007/s12008-022-00841-0
21. Panariello, D., Grazioso, S., Caporaso, T., et al.: Biomechanical analysis of the upper body during overhead industrial tasks using electromyography and motion capture integrated with digital human models. Int. J. Interact. Des. Manuf. **16**, 733–752 (2022). https://doi.org/10.1007/s12008-022-00862-9
22. Ma, L., Ma, R., Chablat, D., Bennis, F.: Human arm simulation for interactive constrained environment design. Int. J. Interact. Des. Manuf. **7**, 27–36 (2013). https://doi.org/10.1007/s12008-012-0162-z
23. Buzzi, M., Colombo, G., Facoetti, G., et al.: 3D modelling and knowledge: tools to automate prosthesis development process. Int. J. Interact. Des. Manuf. **6**, 41–53 (2012). https://doi.org/10.1007/s12008-011-0137-5
24. Gross, M.E.: The GEBODIII program user's guide and description. ALTR-19914102, Armstrong Aerospace Research Laboratory, Wright-Patterson AFB, Ohio (1991)
25. Cheng, H., Obergefell, L., Rizer, A., Directorate, A.L.: (U. S). CS (1994) Generator of Body (GEBOD) Manual. Armstrong Laboratory, Air Force Material Command
26. Cheng, H., Obergefell, L., Rizer, A.L.: The development of the GEBOD program. In: Proceedings of 1996 Fifteenth South Biomedical Engineering Conference, pp. 251–254 (1996)
27. Young, J.W.: Anthropometric and mass distribution characteristics of the adult female. Federal Aviation Administration, Office of Aviation Medicine. Washington, D.C (1983)
28. Cicchella, A.: Development of the biomechanical technologies for the modeling of major segments of the human body: linking the past with the present. Biology (Basel). **9**, 1–13 (2020). https://doi.org/10.3390/biology9110399
29. Smith, S.H.L., Bull, A.M.J.: Rapid calculation of bespoke body segment parameters using 3D infra-red scanning. Med. Eng. Phys. **62**, 36–45 (2018). https://doi.org/10.1016/j.medengphy.2018.10.001
30. Sheets, A.L., Corazza, S., Andriacchi, T.P.: An automated image-based method of 3D subject-specific body segment parameter estimation for kinetic analyses of rapid movements. J. Biomech. Eng. **132**, 1–10 (2010). https://doi.org/10.1115/1.4000155
31. Huang, H.K., Wu, S.C.: The evaluation of mass densities of the human body in vivi from CT scans. Comput. Biol. Med. **6**, 337–343 (1976). https://doi.org/10.1016/0010-4825(76)90070-6
32. Peyer, K.E., Morris, M., Sellers, W.I.: Subject-specific body segment parameter estimation using 3D photogrammetry withmultiple cameras. PeerJ 2015:. (2015). https://doi.org/10.7717/peerj.831
33. Danckaers, F., Huysmans, T., Lacko, D., Sijber, J.: Evaluation of 3D body shape predictions based on features. In: 6th International Conference on 3D Body Scanning Technologies, pp. 258–265 (2015)
34. Ackland, T.R., Henson, P.W., Bailey, D.A.: The uniform density assumption: its effect upon the estimation of body segment inertial parameters. Int. J. Sport Biomech. **4**, 146–155 (1988). https://doi.org/10.1123/ijsb.4.2.146
35. Pascoletti, G., Catelani, D., Conti, P., et al.: Multibody models for the analysis of a fall from height: accident, suicide, or murder? Front. Bioeng. Biotechnol. **7** (2019). https://doi.org/10.3389/fbioe.2019.00419
36. Pascoletti, G., Catelani, D., Conti, P., et al.: A multibody simulation of a human fall: model creation and validation. Procedia Struct. Integr. **24**, 337–348 (2019). https://doi.org/10.1016/j.prostr.2020.02.031
37. Danckaers, F., Huysmans, T., Sijbers, J.: Adaptable digital human models from 3D body scans. DHM Posturogr. (2019). https://doi.org/10.1016/B978-0-12-816713-7.00033-7
38. Obergefell, L., Gardner, T.R., Kaleps, I., Fleck, J.: Articulated Total Body Model Enhancements, vol. 2. User's Guide (1988)
39. Lupker, H.A., de Coo, P.J.A., Nieboer, J.J., Wismans, J.: Advances in MADYMO crash simulations. In: International Congress & Exposition, SAE International (1991)
40. Snyder, R.G.: Anthropometry of infants, children, and youths to age 18 for product safety design. Final report, U.S. Government Printing Office (1977)
41. Mcconville, J.T., Churchill, E., Laubach, L.L., Clauser, C.E., Reardon, J.A.: Anthropometry of air force women. Aerospace Medical Research Laboratory, Wright-Patterson AFB, Ohio (1972)
42. Grunhofer, H.J., Kroh, G.: A review of anthropometric data of German Air Force and United States Air Force flying personnel 1967–1968. Appl. Ergon. **7**, 110–111 (1976). https://doi.org/10.1016/0003-6870(76)90172-1
43. Huysmans, T., Goto, L., Molenbroek, J.F.M., Goossens, R.: DINED mannequin. Tijdschr. voor Hum. Factors. **45**(1), 4–7 (2020)
44. Robinette, K.M., Blackwell, S., Daanen, H., et al.: Civilian American and European surface anthropometry resource (caesar) final report, volume I: summary (2002)
45. Danckaers, F., Huysmans, T., Hallemans, A., et al.: Posture normalisation of 3D body scans. Ergonomics. **62**, 834–848 (2019). https://doi.org/10.1080/00140139.2019.1581262
46. Pascoletti, G., Aldieri, A., Terzini, M., et al.: Stochastic PCA-based bone models from inverse transform sampling: proof of concept for mandibles and proximal femurs. Appl. Sci. (2021). https://doi.org/10.3390/app11115204

47. Allen, B., Curless, B., Popović, Z.: The space of human body shapes: reconstruction and parameterization from range scans. In: ACM SIGGRAPH 2003 Papers SIGGRAPH–03, pp. 587–594 (2003). https://doi.org/10.1145/1201775.882311
48. Drillis, R., Contini, R., Bluestein, M.: Body segment parameters; a survey of measurement techniques. Artif. Limbs. **25**, 44–66 (1964)
49. Erdmann, W.S.: Geometry and inertia of the human body: review of research. Acta Bioeng. Biomech. **1**, 23–35 (1999)
50. Dumas, R., Wojtusch, J.: Estimation of the body segment inertial parameters for the rigid body biomechanical models used in motion analysis (2018)
51. Winter, D.A.: Biomechanics and motor control of human movement. John Wiley & Sons (2009)
52. Dumas, R., Chèze, L., Verriest, J.P. Adjustments to McConville et al. and Young, et al. body segment inertial parameters. J. Biomech. **40**, 543–553. (2007). https://doi.org/10.1016/j.jbiomech.2006.02.013
53. Alsufyani, N.A., Dietrich, N.H., Lagravère, M.O., et al.: Cone beam computed tomography registration for 3-D airway analysis based on anatomic landmarks. Oral Surg. Oral Med. Oral Pathol. Oral Radiol. **118**, 371–383 (2014). https://doi.org/10.1016/j.oooo.2014.05.027
54. Schultz, R.B., Obergefell, L.A., Rizer, A.L., et al.: Comparison of measured and predicted human whole-body inertial properties. SAE Tech. Pap. **106**, 3755–3764 (1997). https://doi.org/10.4271/973332
55. Zatsiorsky, V. M., Seluyanov, V. N., Chugunova, L.G.: Methods of determing mass-inertial characteristics of human body segments. Contemp. Probl. Biomech. 272–291 (1990)
56. Yanagida, Y., Maeda, M., Nushida, H., et al.: Determining falling patterns by estimation of horizontal distance and height. Int. J. Legal Med. **125**, 1–10 (2011). https://doi.org/10.1007/s00414-009-0371-6
57. Cross, R.: Forensic physics 101: falls from a height. Am. J. Phys. **76**, 833–837 (2008). https://doi.org/10.1119/1.2919736
58. Wischhusen, F., Patra, S., Braumann, M., et al.: Analysis of jumping/falling distance from a height. Forensic Sci. Int. **156**, 150–153 (2006). https://doi.org/10.1016/j.forsciint.2004.12.030
59. Happee, R., Nayef, A., Morsink, P., de Lange, R., Bours, R., van Hoof, J.: Mathematical human body models representing a mid size male and a small female for frontal, lateral and rearward impact loading. In: Ircobi, pp. 1–18 (2000)
60. Yang, J.K., Lövsund, P., Cavallero, C., Bonnoit, J.: A human-body 3D mathematical model for simulation of car-pedestrian impacts. J. Crash Prev. Inj. Control. **2**, 131–149 (2000). https://doi.org/10.1080/10286580008902559
61. Yang, J., Mellander, H., Lovsund, P., et al.: A methodology using a combined Injury Criteria Index to study the performance of various driver restraint system configurations. Esv 1–10 (2001)
62. Wismans, J., Happee, R., Van Dommelen, J.A.W.: Computational human body models. Solid Mech. Appl. **124**, 417–429 (2005). https://doi.org/10.1007/1-4020-3796-1_43
63. Happee, R., Hoofman, M., Van Den Kroonenberg, A.J., et al.: A mathematical human body model for frontal and rearward seated automotive impact loading. SAE Tech. Pap. (1998). https://doi.org/10.4271/983150
64. Horst van der, M.J.: Human head neck response in frontal, lateral and rear end impact loading: modelling and validation. Ph.D. Thesis, Technische Universiteit Eindhoven (2002). https://doi.org/10.6100/IR554047